AD-A111 789 JOHNS HOPKINS UNIV LAUREL MD APPLIED PHYSICS LAB F/G 21/5
SUPERSONIC COMBUSTOR INSULATION ABLATION ANALYSIS AND TESTS,(U)
MAY 81 R W NEWMAN, H G FOX

UNCLASSIFIED NL

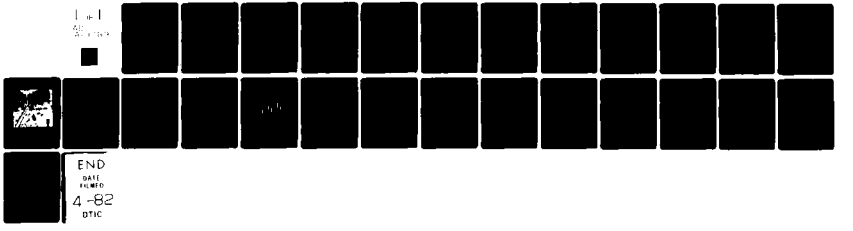

END
DATE FILMED
4-82
DTIC

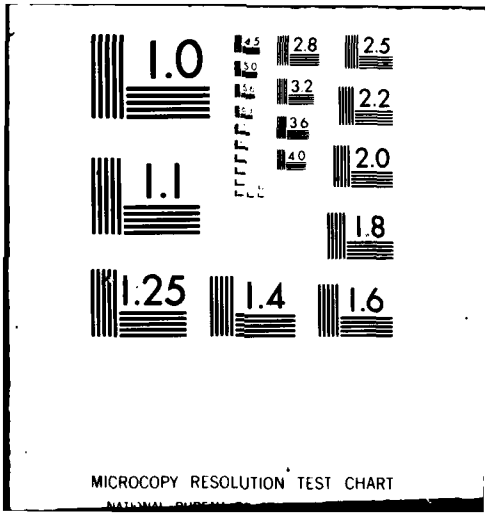
1.0
1.1
1.25
1.4
1.6
1.8
2.0
2.2
2.5
2.8
3.2
3.6
4.0
MICROCOPY RESOLUTION TEST CHART

SUPERSONIC COMBUSTOR INSULATION ABLATION ANALYSIS AND TESTS

Robb W. Newman and Harold G. Fox
Johns Hopkins/Applied Physics Laboratory, Laurel, Maryland

ABSTRACT

14 MAY 81

The design of passively cooled, hypersonic tactical missiles poses many severe structural problems whose solutions are beyond the current state-of-the-art. Specifically, the heating conditions in the supersonic combustor of such a missile approach those in the throat section of rocket motors but are more damaging to most materials because the flow is oxidizing rather than reducing.

Carbon-carbon materials are being considered for the supersonic combustor wall structure because they have attractive strength-weight characteristics at elevated temperatures. Since these materials have poor oxidation resistance, metal loaded carbon-carbon materials which form an oxidation resistant layer are also being considered. In order to design such a combustor, the designer must be able to accurately predict the erosion rate of candidate materials so that a realistic balance can be achieved between weight and performance. This paper addresses the problem of thermochemical erosion of graphitic materials, the development of procedures for the analytic prediction of these erosion rates in a combustor environment, and experimental procedures used to validate the analytical model and evaluate candidate combustor liner materials.

INTRODUCTION

Previous reviews and evaluations of graphite ablation theory and experimental data[1,2] have been conducted for blunt body atmospheric reentry analyses as part of the Aerospace Nuclear Safety Program. Although these references are slanted to environmental conditions and configurations entirely different than those under consideration herein, the basic theory and simplified model are applicable. Therefore, it was the objective of this study to modify the existing model in order to consider the oxidation of graphite wall materials in the presence of a supersonic combustor environment during a flight profile.

During the powered flight portion of the ramjet trajectory, the fuel is burned in varying mass ratios with air, releasing heat and by-products in the combustor chamber. The resulting high temperature gas mixture flows through this pipe-like configuration at supersonic velocities while transferring heat to the combustor wall. The heat transfer rate at this interface has been determined from an empirical correlation which will be discussed later.

In review, the basic ablation process occurs as follows:

When the wall temperature reaches a certain level, which depends on the surface material's reactivity, a heterogeneous chemical reaction (oxidation) between the hot boundary layer and the surface material ensues. In this first "reaction-rate controlled" regime, the surface oxidation rate increases exponentially with surface temperature (e.g., by an Arrhenius kinetic mechanism). Reaction-rate control

persists with increasing surface temperature until the diffusional transport of oxident to the surface becomes too slow to maintain the exponential increase in reaction rate. This "transition regime" extends to the temperature level where the surface reaction becomes completely diffusion controlled. At this condition, the reaction is said to be in the diffusion-limited regime and is characterized by surface oxidation occurring in stoichiometric proportions (the stoichiometry depending on the products formed). As the surface temperature continues to increase, the oxidation rate remains diffusion-limited until a critical temperature/pressure condition is reached at which the graphitic material also begins to sublime. In this sublimation regime the mass loss rate again increases exponentially with surface temperature as dictated by the partial pressure of the vaporizing carbon species.

For our combustor ablation model, the sublimation regime has been neglected. This simplification has been assumed because sublimation of graphite materials have been observed to begin at approximately 5500°R, which is a temperature well above the maximum expected surface temperature under consideration for the trajectories presently being evaluated.

THE REACTION-RATE CONTROLLED (KINETIC) REGIME

Experimental surface reaction rate data are normally presented in the Arrhenius plane, i.e., $\log m_r$ vs $1/T$, in an attempt to correlate the data with the empirical Arrhenius rate equation,

$$m_r = P_{O_w}^{n} k_o \exp(-E/RT_w) \qquad (1)$$

where m_r is the carbon mass loss rate, k_o is the "frequency factor" or "reaction rate constant", n is the order of the reaction, E is the activation energy, and P_{O_w} is the partial pressure of the oxidant at the surface.

Scala[3] in an attempt to bracket the available data on graphite, utilized a set of "slow" and "fast" values for E and k_o with $n = 1/2$. Subsequently Metzger[4], based on the experimental arc-jet data on ATJ, formulated a third set that resulted in rates between the "fast" and "slow" values of Scala and labeled as the 'moderate' rates. The resulting values are:

$k_o = 9.65 \times 10^5$ lb/(ft^2 - sec-atm$^{1/2}$)

E = 44,000 cal/mol

R = 1.98718 cal/mole - °K (universal gas constant)

T_w = wall temperature, °K

Presently, there are no reported experimental data on carbon-carbon to arrive at similar reaction constant values for this material. Therefore, the above values for ATJ graphite are employed as the first approximation for the E and k_o of carbon-carbon for our present model.

Nagle[5] and Strickland-Constable[6] have reported rate constants for the oxidation of pyrolytic graphite (PG). They fit their experimental data to a surface reaction mechanism proposed by Blyholder, Binford, and Eyring[7]. The mechanism was developed to explain the observation that the oxidation of PG appears to follow at

least two different rate equations. At temperatures below 1000°K (1340°F), the oxidation can be described by a rate equation with an activation energy of 25 to 30 kcal/gmole. The rate of oxidation reaches a maximum in the region between 1000 and 1700 K (1340 to 2600°F), then decreases, and at still higher temperatures again increases with an activation energy from 70 to 90 kcal/gmole.

It is assumed that two types of surface active sites are present on PG. Type A sites, the more reactive sites, support the oxidation reaction at low temperatures. At higher temperatures some Type A sites are converted to less reactive type B sites, accounting for the temporary decrease in the oxidation rate in the intermediate range of temperatures. This mechanism is described by a set of three elementary reactions wherein CO is assumed to be the only product:

(i) $A + O_2 \rightarrow A + 2CO$ $\quad \dot{m}_r\ (i) = k_A P_{O_w} X / \left(1 + k_z P_{O_w}\right)$

(ii) $B + O_2 \rightarrow A + 2CO$ $\quad \dot{m}_r\ (ii) = k_B P_{O_w} (1-X)$

(iii) $A \rightarrow B$ $\quad \dot{m}_r\ (iii) = k_T X$

where

X = Fraction of surface covered with Type A sites

$(1-X)$ = Fraction of surface covered with Type B sites

P_{O_w} = Partial pressure of oxygen, atm ($= P_w \cdot \Phi_{O_2}$)

Φ_{O_2} = Mole fraction of oxygen

k_A, k_B, k_z, k_T = constants

where

$$X = \frac{k_B P_{O_w}}{k'_B P_{O_w} + k_T} \tag{2}$$

The total rate of reaction is

$$\dot{m}_r = \frac{k_A P_{O_w}}{1+k_z P_{O_w}} X + k_B P_{O_w} (1-X) \tag{3}$$

in gram atoms carbon/cm^2-sec. Values for the reaction rate constants were obtained by finding those values which best fit the experimental data:

k_A = 20 exp (-30,000/RT) gram-atoms/(cm^2-sec-atm)

k_B = 4.46 x 10^{-3} exp (-15,200/RT) gram-atom/(cm^2-sec-atm)

k_T = 1.51 x 10^5 exp (-97,000/RT) gram-atom/(cm^2-sec)

k_z = 21.3 exp (+4,100/RT) 1/atm

TRANSITION AND DIFFUSION LIMITED REGIMES

In the transition regime the mass loss rate is computed from,

$$\frac{\dot{m}}{\dot{m}_D} = \frac{1}{2} + \left[\frac{1}{4} + \frac{\dot{m}_D}{\dot{m}_r}^2\right]^{1/2}{}^{-1} \qquad (4)$$

which is a 1/2-order reaction (Reference 1) and where $\dot{m}_D$ is the mass loss rate in the diffusion-limited regime.

The evaluation of graphite surface ablation throughout all the thermochemical regimes is summarized by the non-dimensional oxidation term called the "mass transfer parameter", β, which is defined as

$$\beta' = \dot{m}/\rho u C_h \qquad (5)$$

where

$\dot{m}$ = the mass loss rate

$\rho u C_h$ = heat transfer coefficient

C_h = Stanton Number

and for the diffusion limited regime

$$\beta_D' = \dot{m}_D / (\rho u C_h) \qquad (6)$$

Equation (6) can be re-arranged to obtain the $\dot{m}_D$ from the "diffusion limited mass transfer parameter", β_D'

$$\dot{m}_D = (\rho u C_h)\, \beta_D' \qquad (7)$$

where $(\rho u C_h)$ and β_D' can be independently determined, which will be discussed later.

The mass loss rate equations for each of the thermochemical regimes are combined by means of the Mickley-Spalding blowing relation[8] to form the following equation to determine β' (which is essentially the solid carbon to free stream gas mixture mass ratio),

$$\beta' = (1 + \beta_D')^{\dot{m}/\dot{m}_D} - 1 \qquad (8)$$

REACTIVITY OF CARBON

At elevated temperatures, and, to a first approximation, irrespective of the nature of the carbon, the reactivity is the greatest in oxygen and least in hydrogen, as summarized in Table 1 (Reference 9). This table also reveals that the $C + O_2$ reaction is roughly 10^5 times as fast as the $C + CO_2$ reaction at around $1900^\circ R$. Based on this finding, our model assumes that the carbon wall reacts only with the O_2 remaining in the by-products of the Shelldyne-H/air* mixture and CO

*Shelldyne-H is the fuel under consideration. See Appendix A for properties.

is the only by-product of the solid carbon reaction according to

$$2C + O_2 \rightarrow 2CO \qquad (9)$$

Table 1

Approximate Relative Rates of Carbon + Gas Reactions at 1931°R and 0.1 Atm

Reaction	Relative Rates
$C + CO_2$	1
$C + O_2$	1×10^5
$C + H_2O$	3
$C + H_2$	3×10^{-3}

DIFFUSION-LIMITED MASS TRANSFER PARAMETER (β_D')

The diffusion-limited mass transfer parameter, β_D', is essentially the solid carbon to free stream gas mixture mass ratio at stoichiometric proportions. With the assumption that the solid carbon only reacts with the O_2 in the free stream and CO is the only by-product, the basic reaction equation is

$$C + \frac{1}{2(0.21 - 0.198ER)} \frac{M_a}{M_f} \cdot f_s \cdot ER \cdot C_{14} H_{18} + 0.198 \cdot ER \cdot O_2 + 0.79 \cdot N_2 +$$

$$(0.21 - 0.198 \cdot ER)\ O_2 \rightarrow CO + (\text{Shelldyne H/air less } O_2) \qquad (10)$$

The relationship defining β_D' as a function of the fuel/air equivalence ratio (ER) can be derived with the utilization of this reaction equation. After further rearrangement of terms and the substitution of molecular weights, the β_D' equation reduces to

$$\beta_D' = \frac{(0.1748 - 0.1648\ ER)}{(1.0 + 0.0730\ ER)} \qquad (11)$$

Figure 1 presents the variation of β_D' versus ER per equation (11). When the ER equals zero, the β_D' is essentially equal to the diffusion limited value for air (0.1748).

COMBUSTOR HEAT TRANSFER CORRELATION

Over many years of combustor testing at APL, heat transfer measurements have been taken for varied geometries and different fuels. It has been the intent of this data gathering exercise to correlate the average heat flux values from these tests against a heat release parameter which is proportional to the effective equivalence ratio (ER_{eff}) for any given fuel. This heat release parameter is

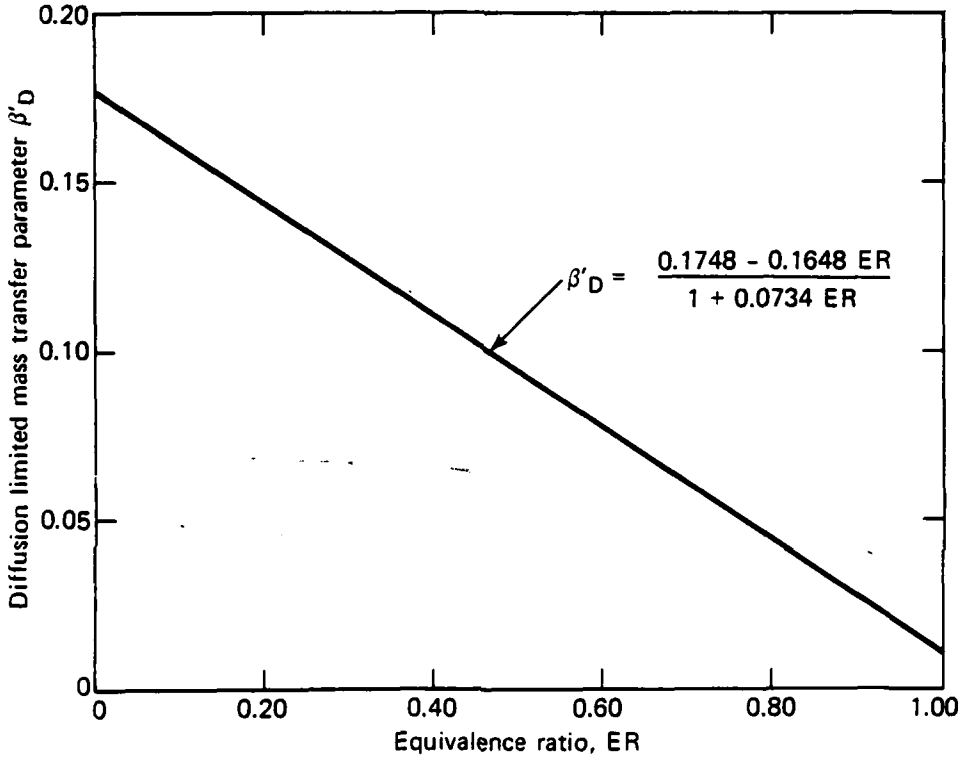

Fig. 1 Diffusion limited mass transfer parameter.

equal to the product of the fuel-air ratio (f), the lower heating value of the fuel (h_f), and the combustor efficiency (η).

Figure 2 (from Reference 10) presents the correlation of the normalized wall heat flux parameter as a function of the heat release parameter (the ER_{eff} scale for Shelldyne-H is also included.) The normalized wall heat flux parameter is equal to

$$(q_w/A_w)/\left(\frac{\dot{w}_a \Delta h}{A_{c_i}}\right)$$

where:

q_w = Wall heat flux

A_w = Wall area

A_{c_i} = Combustor inlet area

$\dot{w}_a$ = Air mass flow rate

Δh = Average gas to wall enthalpy difference

Noting that by definition

$$\rho u C_h \simeq (q_w/A_w)/\Delta h \qquad (12)$$

the combustor heat transfer coefficient can be determined for any air mass flow rate ($\dot{w}_a$) and a specific combustor geometry cross sectional area (A_{c_i}) from this empirical correlation instead of an analytical approximation such as Bartz[11].

The air mass flow rate in the supersonic combustor is determined from the continuity equation in the following form,

$$w_a = P_w A_c M \left(\frac{g\gamma}{RT_g}\right)^{1/2}$$

where

P_w = Pressure at the wall

A_c = Cross-sectional area of combustor

M = Mach Number

R = Air mixture gas constant

T_g = Average total temperature of the air mixture

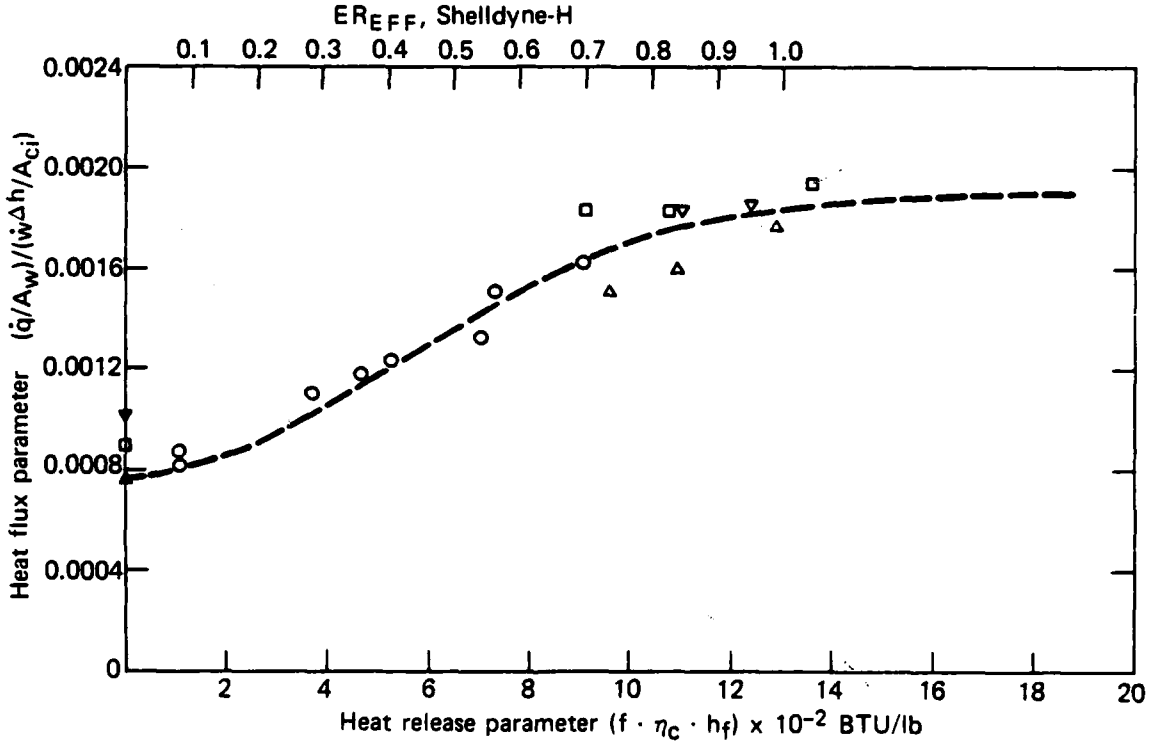

Fig. 2 Correlations of wall heat-flux parameter with heat-release parameter.

THERMOCHEMISTRY DATA DETERMINATION

The thermochemical erosion of graphite materials is dependent on information denoted as thermochemistry data. This data consists of the mass transfer parameter (β') and the enthalpy of the gas mixture at the graphite wall interface (h_w) tabulated for different wall temperatures (T_w) and pressures (P_w). The ablation model reviewed in the previous sections is now utilized to calculate the β' for varying T_w and P_w for a specific supersonic combustor design and fuel equivalence ratio (ER).

A basic procedure leading to the calculated β' is:

1. For the desired ER, the β'_D and the oxygen mole fraction of the by-products mixture can be determined for the Shelldyne-H/air fuel mixture (See Appendix A for Shelldyne-H properties);

2. For the specific combustor design (A, M, T_g), the air mass flow rate can be determined for varying P_w;

3. The heat transfer coefficient between the free stream gas mixture and the combustor wall can then be determined from the heat flux correlation for the ER and w_a;

4. The mass loss rates for each of the thermochemical regimes (depending on PG or C/C) is determined for varying T_w and P_w;

5. β' can be determined.

The relationship between β', h_w, T_w, P_w is generated by means of a thermochemical computer code (NOTS)[12]. The calculations are based on equilibrium thermochemistry where solid carbon is the fuel reacting with the hydrogen, carbon, nitrogen, and oxygen constituents of the gas mixture. Twenty-one species have been considered in the equilibrium calculation in which their thermochemical data are from the JANNAF tabulations where all enthalpies are referred to the base at 298.16°K, 1 atm and the elements in their natural state.

COMPUTER PROGRAM

The above procedure has been incorporated into a computer program. A new version of the NOTS (NOTS-CMA)[12] code has been created with modifications and the addition of a subroutine for the sole purpose of generating the thermochemistry data in the proper input format for the heat transfer analysis computer program CMA[13].

Figure 3 presents the calculated β' for various Shelldyne-H ER's over carbon-carbon material. In each case, the β' levels off at the diffusion limited value. For any specific ER, the effect of P_w on β' is negligible above 2500°R. However, for the case of Shelldyne-H over PG, its an entirely different result. Figure 4 presents the β' for the ER = 0.5 case showing, not only a variation with wall pressure, but, more importantly, the mass transfer parameter reaches a maximum in the temperature range of 3500-4000°R then drops. The oxidation of PG is kinetically controlled (not diffusion limited) and behaves in a peculiar manner per the previous discussion. Since CMA requires that the

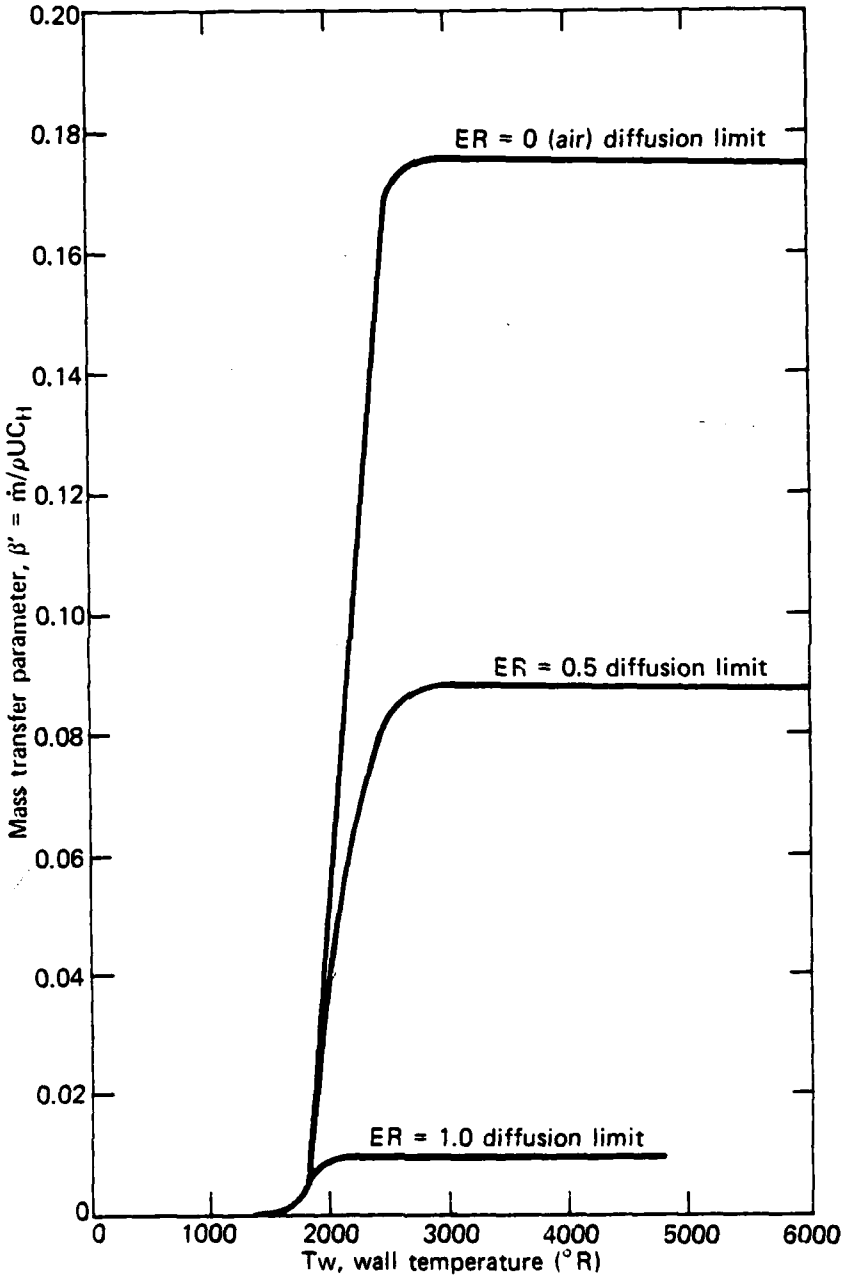

Fig. 3 Carbon oxidation comparison of transition region, 1 atm pipe configuration, 0.795 ft dia., carbon-carbon, Shelldyne - H/air.

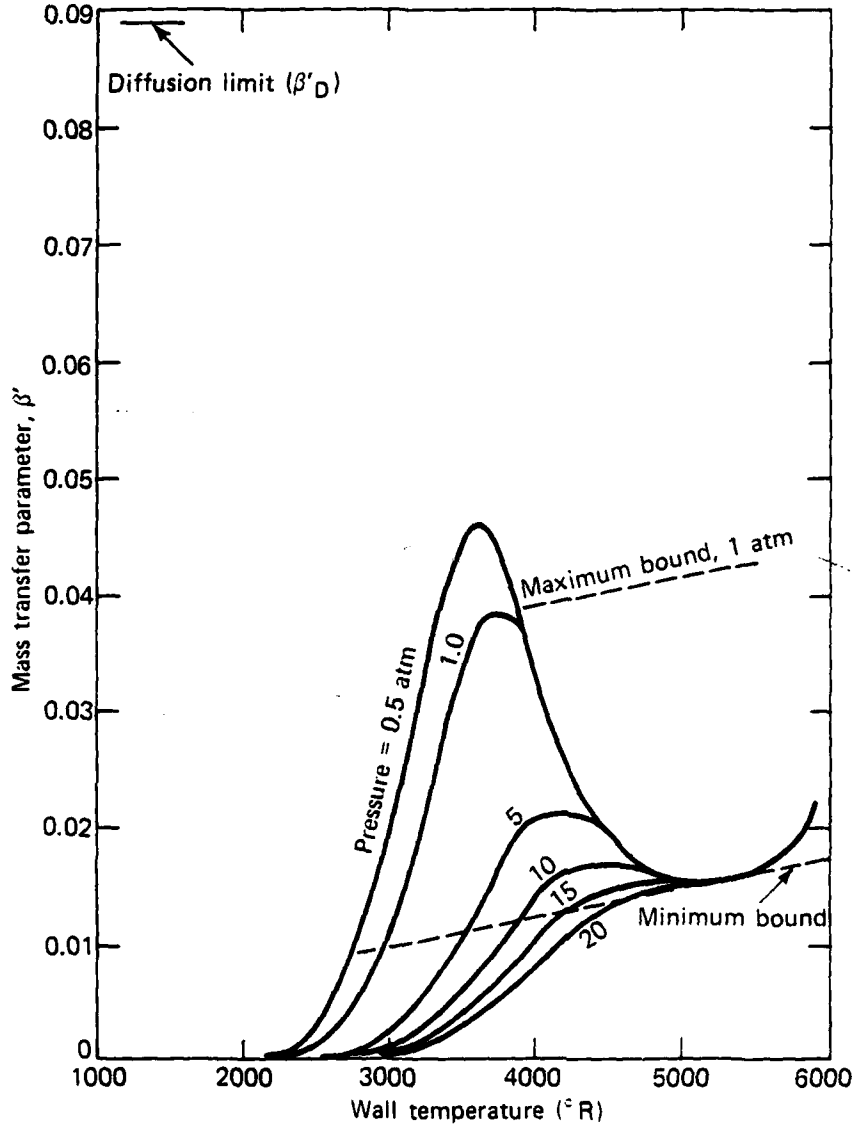

Fig. 4 Mass-transfer parameter versus wall temperature for various pressures. Shelldyne · H, ER = 0.50, PG wall.

β' versus T_w be monatonically increasing, β' is bounded at a maximum and minimum slope as shown in Figure 4 and a range of surface ablation is calculated.

EXPERIMENTAL RESULTS

The development of high performance supersonic combustor materials requires an understanding of the mechanical and chemical processes taking place at the ablating surface of various materials. This is impossible to obtain from analysis alone and requires some experimentation. Consequently a series of tests were performed at the McDonnell Douglas High Impact Pressure (HIP)[14] arc heater facility to simulate sea level and high altitude cruise conditions in a supersonic combustor.

The purposes of these tests were to evaluate candidate supersonic combustor materials and to obtain mass loss and surface temperature data for comparison with analysis. A total of 40 models were tested, with each model nominally 0.5 inches wide by 0.5 inches thick by 1.25 inches long. A model was placed on each arm of an eight arm turret (Figures 5 and 6) and injected into the arc jet. Thirty-two of the models were tested at a 10^{o} angle-of-attack for 75 s each at a nominal brightness temperature of $5000^{o}R$ (ε=1) using a similated Shelldyne - air mixture to approximate high altitude cruise conditions. Eight models were tested for 40 s at a 25^{o} angle-of-attack using a Shelldyne - air mixture to simulate sea-level conditions. Surface brightness temperature was measured at four locations along the model centerline (0.25, 0.55, 0.85 and 1.15 inches from the leading edge) using optical pyrometers. The model backface temperature history was measured at the 0.85 inch position using a tungsten-rhenium thermocouple. Model recession histories were obtained from 16 mm movie films of the model profile.

Several materials were used to determine which were best suited for scramjet engine combustors. Particular interest was given to metal impregnated carbon-carbon (C-C) materials which in theory form protective metal oxide layers, retained at the surface by high viscosity silica compounds also added to the specimens. A summary of the processing treatments and composition of metal and silica additives for each specimen is presented in Table 2. In addition, some reference materials including virgin C-C, pyrolytic graphite (PG) coated C-C, pyrolytic graphite/silicon carbide (PG/S-C) coated ATJ graphite, and ATJ-S graphite were also used.

A summary of the mass recession loss rate results is presented in Figure 7 for the long-range, high altitude tests and Figure 8 for the sea-level test. In the high-altitude tests there is no particular trend in the metal additive composition or process and there appears to be no benefit from metal additives. On the contrary, the limited data suggests metal additives have increased the recession rate. Except for model #21 (ZR(.6) - Si(.2) - B(.2)/RH), the pyrolytic graphite is clearly superior.

The recession rates for materials tested at the sea-level condition show that the metalized C-C samples (24, 14 and 2) are the same or worse than the plain C-C sample number 45. Moreover, PG and PG/SiC had much lower recession rates. Although it appears that the metalized C-C materials offer no significant improvement over other combustor materials, shear stresses on the surface were slightly higher than desired and may have altered the performance that these materials would experience in a real combustor application.

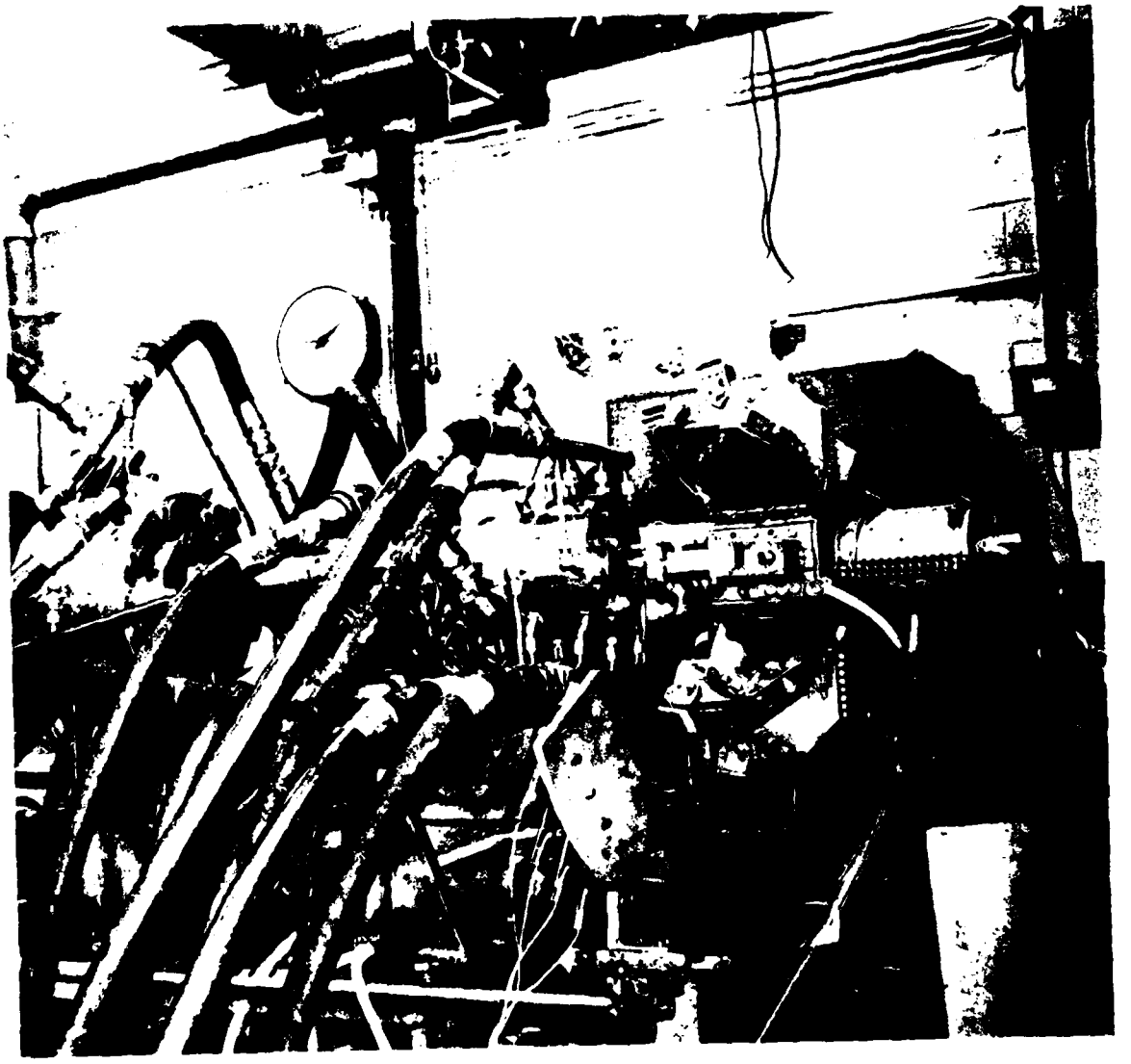

Fig. 5 Typical arc heater and wedge model set-up.

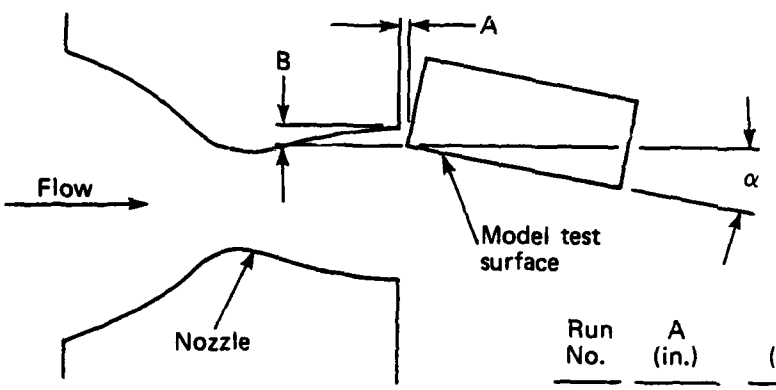

Run No.	A (in.)	B (in.)	α (deg)
1554	0.050	0.100	10
1555	0.050	0.100	10
1558	0.020	0.100	10
1559	0.020	0.100	10
1564	0.050	0.000	25

Fig. 6 Profile view of model (top camera).

Table 2 Material Specimen Number Identifications for HIP Tests

Metallic Additives Composition[+,++]	Processing Precursor and Phase					
	AH	AL	RH	RL	RO	AO
Zr(.6)-Si(.2)-B(.2)	15	(16)	(21)	(23)	(37)	(39)
		17	22	[24]	38	40
Zr(.8)-Si(.1)-B(.1)	(13)					
	[14]					
Zr(.6)-Si(.2)-Ti(.2)	(25)					
Zr(.8)-Si(.1)-Ti(.1)	(18)					
	19					
Hf(.6)-Si(.2)-B(.2)						
Hf(.8)-Si(.1)-B(.1)	(1)					
	[2]					
Hf(.6)-Si(.2)-Ti(.2)	(9)					
Hf(.8)-Si(.1)-Ti(.1)	(7)					

Non-metallized specimens (pitch only) are [45], (47), (48)

Code

AH = Alkoxy - HiC
AL = Alkoxy - LoC
RH = Resinate - HiC
RL = Resinate - LoC
RO = Resinate - Oxide
AO = Alkoxy - Oxide

( ) - Runs 1554 & 1555
⬡ - Runs 1558 & 1559
[ ] - Run 1564

+Numbers in parentheses refer to mole fraction of the metal additive.
++Materials are listed from top to bottom in order of increasing theoretical refractoriness.

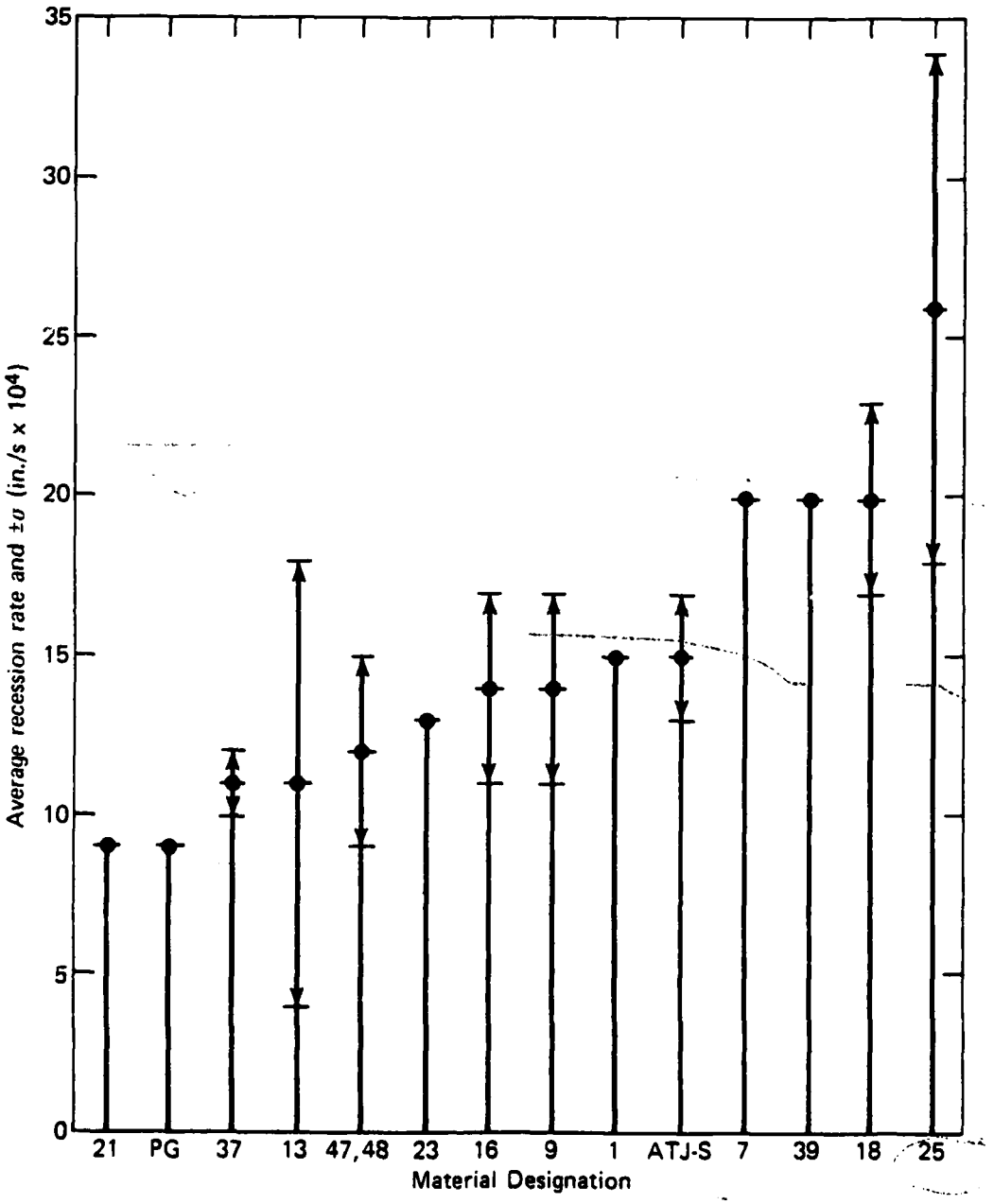

Fig. 7 Material recession rate performance for high-altitude tests.

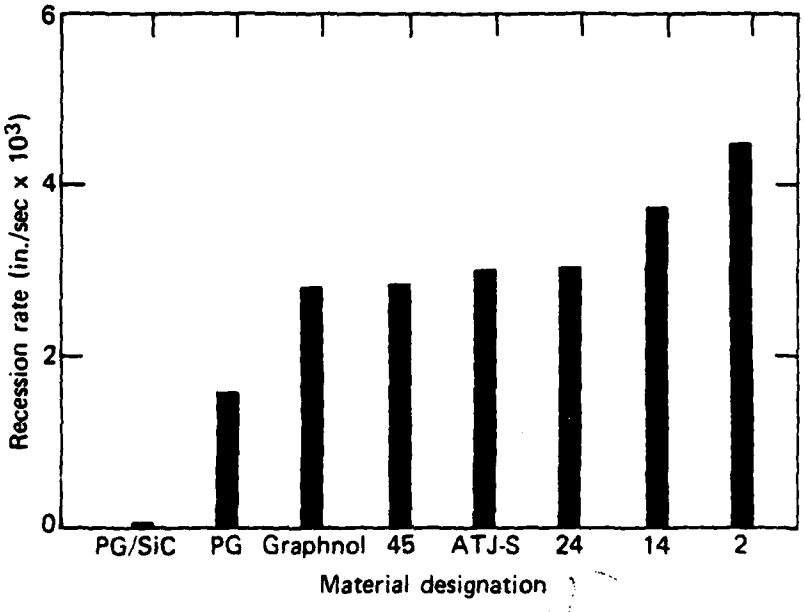

Fig. 8 Material recession rate performance for sea-level tests.

COMPARISON OF MEASURED AND PREDICTED MATERIAL RECESSION

Results from the HIP tests have been compared with predicted analytical values of recession and surface temperature and agree to within 25%. The test conditions analyzed were for an ATJ-S specimen placed at a 3.5^{o} angle of attack in air at $5620^{o}R$ at simulated high altitude cruise conditions. Thermochemical properties of carbon-carbon were obtained from the EST computer code[15] assuming no CO_2 in the chemically reacting products near the ablating surface. The rational for this assumption is based on the fact that the $(2C + O_2 \rightarrow 2CO)$ reaction rate is much faster than the $(2CO + O_2 \rightarrow 2CO)$ reaction rate which in turn, is much faster than the $(2CO + O_2 \rightarrow 2CO)$ rate. Consequently, CO is produced and then swept away from the reacting surface before it has a chance to react with O_2, to form CO_2.

The analytical model consists of a 0.5 inch thick piece of ATJ-S, insulated from a 0.5" steel support by a 0.02" layer of zirconium dioxide (Figure 9). Measured surface temperatures were obtained from black body optical pyrometer temperatures assuming an ATJ-S surface emissivity of 0.78 at 0.9μ.

Predicted surface temperatures compare favorably with optically measured temperatures during the first 20 to 30 seconds of the test (Figure 10). After this time however, measured temperatures decrease sharply and are no longer in good agreement with predicted temperatures which continue to increase. The reason for this is that as the specimen ablates it recedes out of the freejet main stream and into the cooler boundary layer. Therefore, only the first 20 to 30 seconds of the test are a valid simulation of actual combustor conditions, and data taken after that should be ignored.

Surface ablation rates measured during this test, compare well with predicted recession rates throughout the test (Figure 11). Both experiment and analysis indicate ablation begins between 6 and 11 seconds and continues at a constant rate throughout the test. Constant recession rates of 0.0027 and 0.0024 inches/sec have been measured and compare with a slightly higher predicted rate of 0.003 inches/sec. The somewhat surprising aspect of this data is that measured recession rates remain constant even at times greater than 30 seconds, when the surface temperature is decreasing and the heated surface is moving into the freejet boundary layer. This seemingly inconsistent behavior can be explained as follows: In general, ablation rate is expressed as $\beta' \cdot \rho u C_h$ (Equation 7), where β' is the diffusion mass flux ratio expressed as a function of the material, its surface temperature and pressure, while $\rho u C_h$ is the enthalpy based heat transfer coefficient. For ATJ-S the ablation rate is diffusion limited at temperatures above $2400^{o}R$, which means β' is constant about $2400^{o}R$. Since surface temperatures remain above $2400^{o}R$ for most of the test (Figure 10), β' is a constant. However, in order to have a constant recession rate, $\rho u C_h$ must also be constant. Apparently, as the surface recedes into the cool thermal boundary layer, the effect of decreasing stream velocity (u) is offset by a decrease in the reference length, since the effective distance to the leading edge is decreasing as the leading edge leaves the freejet main stream. The good agreement between experimental and analytical surface temperatures and ablation rates give us added confidence in our analytical model.

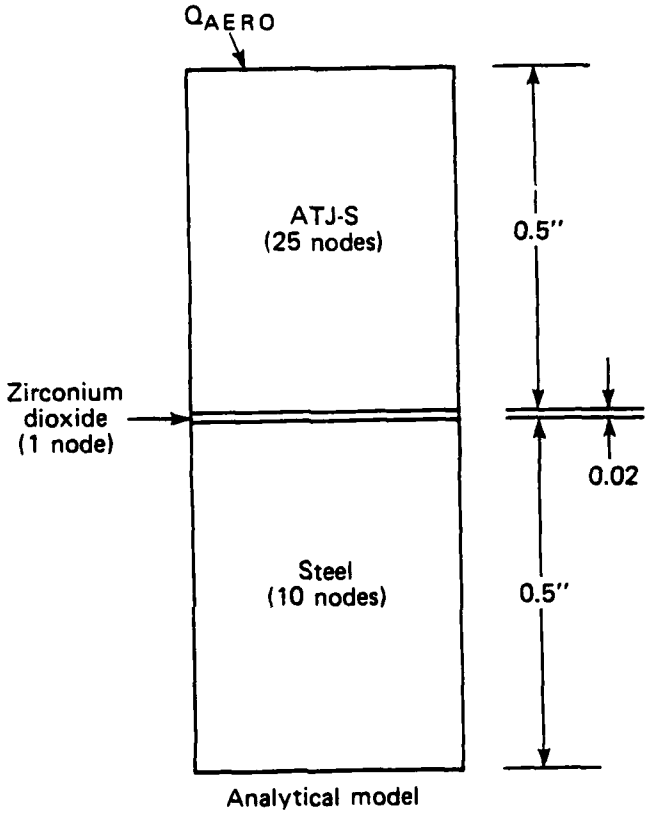

Fig. 9 HIP test specimen.

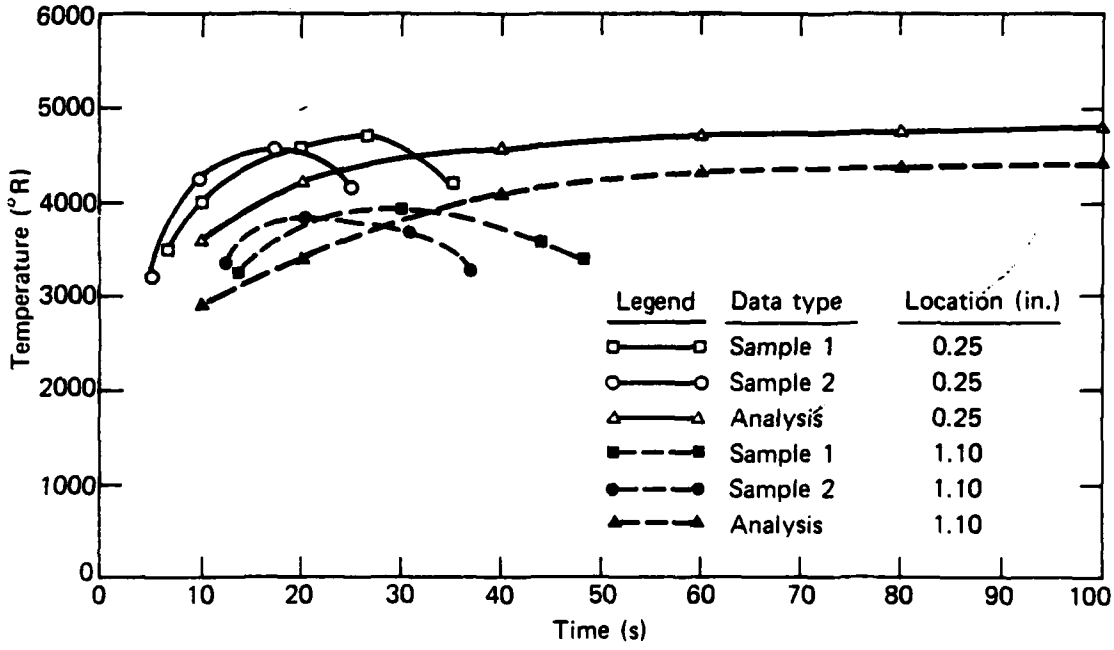

Fig. 10 Comparison of test and analysis surface temperature histories ATJ-S.

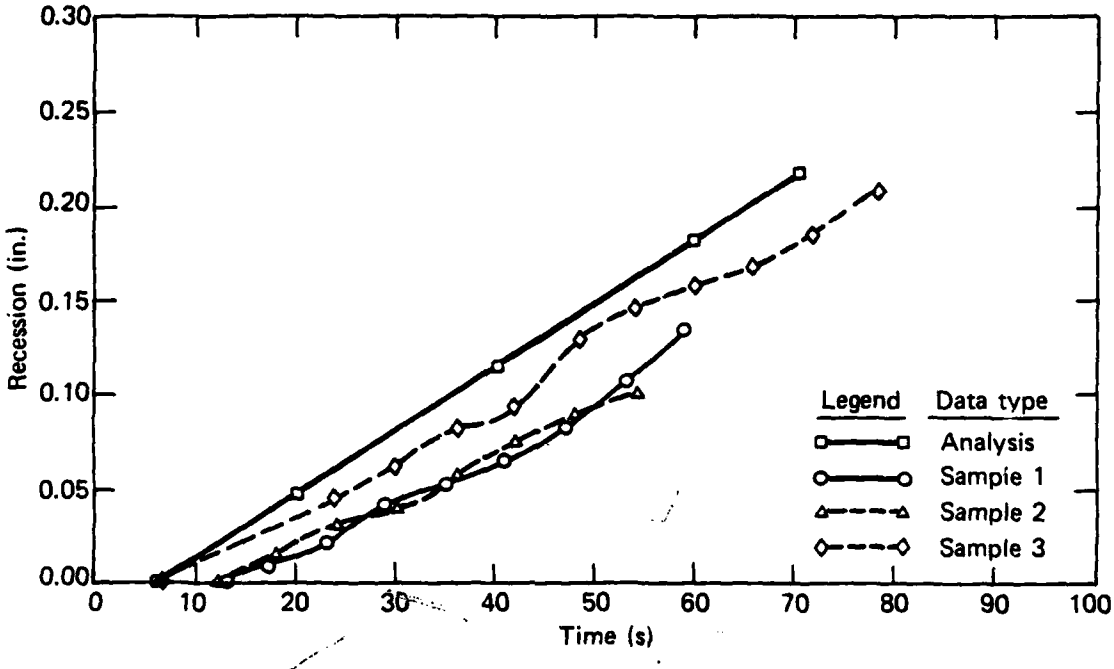

Fig. 11 Comparison of test and analysis ablation histories ATJ-S, 0.85 in. location.

ACKNOWLEDGEMENTS

The thermal ablation computer program development was supported by the Structures & Aerodynamics Block (Mr. L. Pasiuk(SEA 62R) and Dr. Frank Moore (NSWC)) and the materials development was supported by the Materials Block (Mr. M. A. Kinna (SEA 62R)). The metallized carbon-carbon materials were developed and fabricated by the General Electric Re-Entry & Environmental Systems Division (Dr. J. J. Gebhardt) and the experimental test program conducted by the McDonnell Douglas Astronautics Company - St. Louis Division (Messrs. W. A. Rinehardt, R. A. Williamson and J. A. Grace).

REFERENCES

1. Perini, L. L., "Review of Graphite Ablation Theory and Experimental Data", APL/JHU ANSP-M, Dec. 1971.

2. Perini, L. L., "Graphite Oxidation Modeling in Subsonic Flow", APL/JHU ANSP-111, Aug. 1977.

3. Scala, S. M. and Gilbert, L. M., "Aerothermal Behavior of Graphite at Elevated Temperatures", GE Report No. R635D81, Nov. 1963.

4. Metzger, J. W., Engel, M. J., and Diaconis, N. S., "The Oxidation and Sublimation of Graphite in Simulated Re-entry Environments", AIAA No. 65-643, 1965.

5. Nagle, J. and Strickland-Constable, R. F., "Oxidation of Carbon Between 1000-2000°C", Proc. Fifth Conference on Carbon, 1961.

6. Strickland-Constable, R. F., "Theory and the Reaction of Graphite with Oxygen in the Temperature Range 1000-2400°C", 2nd Conference on Industrial Carbon and Graphite, Soc. Chem. Ind. (London), 1966.

7. Blyholder, G., Binford, J. S. and Eyring, H., "A Kinetic Theory for the Oxidation of Carbonized Filaments", J. Phys. Chem., pp. 62, 263, 1958.

8. Mickley, H. S., Ross, R. C., Squyers, A. L., and Stewart, W. E., "Heat, Mass, and Momentum Transfer for Flow Over a Hot Plate with Blowing or Suction", NACA TN-3208, July 1954.

9. Thomas, J. M., "Reactivity of Carbon: Some Current Problems and Trends", Carbon 1970, Vol. 8, pp. 413-421, Pergamon Press.

10. Funk, J. A. Waltrup, P. J., "Wall Heat Flux Correlations for Scram Combustion and Nozzles", Section 11 (U) Quarterly Report, April-June 1977, APL/JHU C-RQR/77-2 (Confidential).

11. Bartz, D. R., "A Simple Equation for Rapid Estimation of Rocket-Nozzle Convective Heat Transfer Coefficients", Jet Prop., pp. 99, Jan. 1957.

12. D. R. Cruise, "Notes on the Rapid Computation of Chemical Equilibria", Journal of Physics and Chemistry, Vol. 68 No. 12 (Dec 1964), pp. 3797-3802.

13. "User's Manual, Aerotherm Charring Material Thermal Response and Ablation Program, Version 3", (CMA), Vol. I and Vol. II, Aerotherm Report No. UM 70-14, April 1970.

14. W. A. Rinehart, R. A. Williamson and J. A. Grace, "Supersonic Combustor Materials Screening in the HIP Arc Heater Facility", McDonnell Douglas Company, St. Louis Division, MDC E2216.

15. "User's Manual, Aerotherm Equilibrium Surface Thermochemistry Program", Version 3, Aerotherm Corporation, Mountain View, California, Report UM-70-13, May 1970.

Appendix A

Shelldyne-H Fuel Properties

The ramjet fuel under consideration for the hypersonic missile is the hydrocarbon fuel, Shelldyne-H (C_{14} H_{18}). Some of its basic properties are:

Density	=	67.5 #/ft^3
Stoichiometric fuel-air ratio (f_s)	=	0.072832
Lower heating value	=	17,890 Btu/#

Table A-1 presents a tabulation of the mole percent of various by-products of combustion for varying equivalence ratio (ER) of the Shelldyne-H/air mixture. The mole percent of O_2 by-product versus ER is plotted for two different free stream air total temperatures of 1080°R and 3780°R in Figure A-1. The approximate curve fit of oxygen mole function for use in our analytical model is

$$(\Phi O_2)\text{moles} = 0.21 - 0.198\ ER$$

which is also plotted in Figure A-1 for comparison.

Figure A-2 presents the variation of combustor total gas temperature versus free stream air total temperature for varying equivalence ratio.

Table A-1

Mole Percent of Products of Combustion
Shelldyne-H + Air

ER	0	.3	.4	.5	.6	.7	.8	.9	1.0
T°R	1080	2438	2830	3197	3539	3845	4098	4281	4392
O_2	21.0	14.45	12.28	10.1	7.9	5.8	3.9	2.32	1.20
N_2	79.0	77.78	77.35	76.9	76.4	75.8	75.2	74.4	73.5
CO_2	0	4.70	6.23	7.74	9.2	10.6	11.6	12.1	11.96
CO	0	0	0	0	.03	.17	.58	1.46	2.87
H_2O	0	3.02	4.0	4.96	5.9	6.8	7.54	8.25	8.85
H	0	0	0	0	0	.01	.02	.06	.11
HO	0	0	0	.034	.10	.22	.37	.50	.54
O	0	0	0	0	.01	.04	.09	.12	.12
NO	0	.05	.14	.28	.45	.59	.66	.63	.50
H_2	0	0	0	0	0	.02	.07	.17	.36

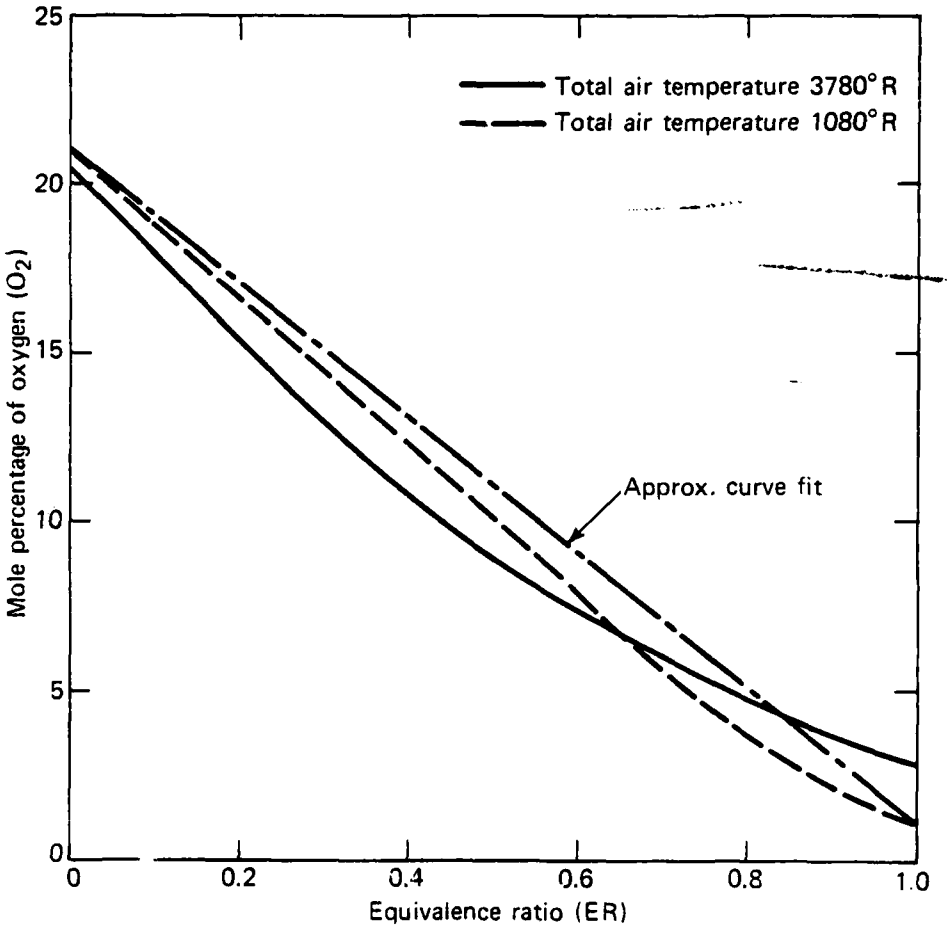

Fig. A-1 Mole percentage of oxygen in Shelldyne - H/air mixture.

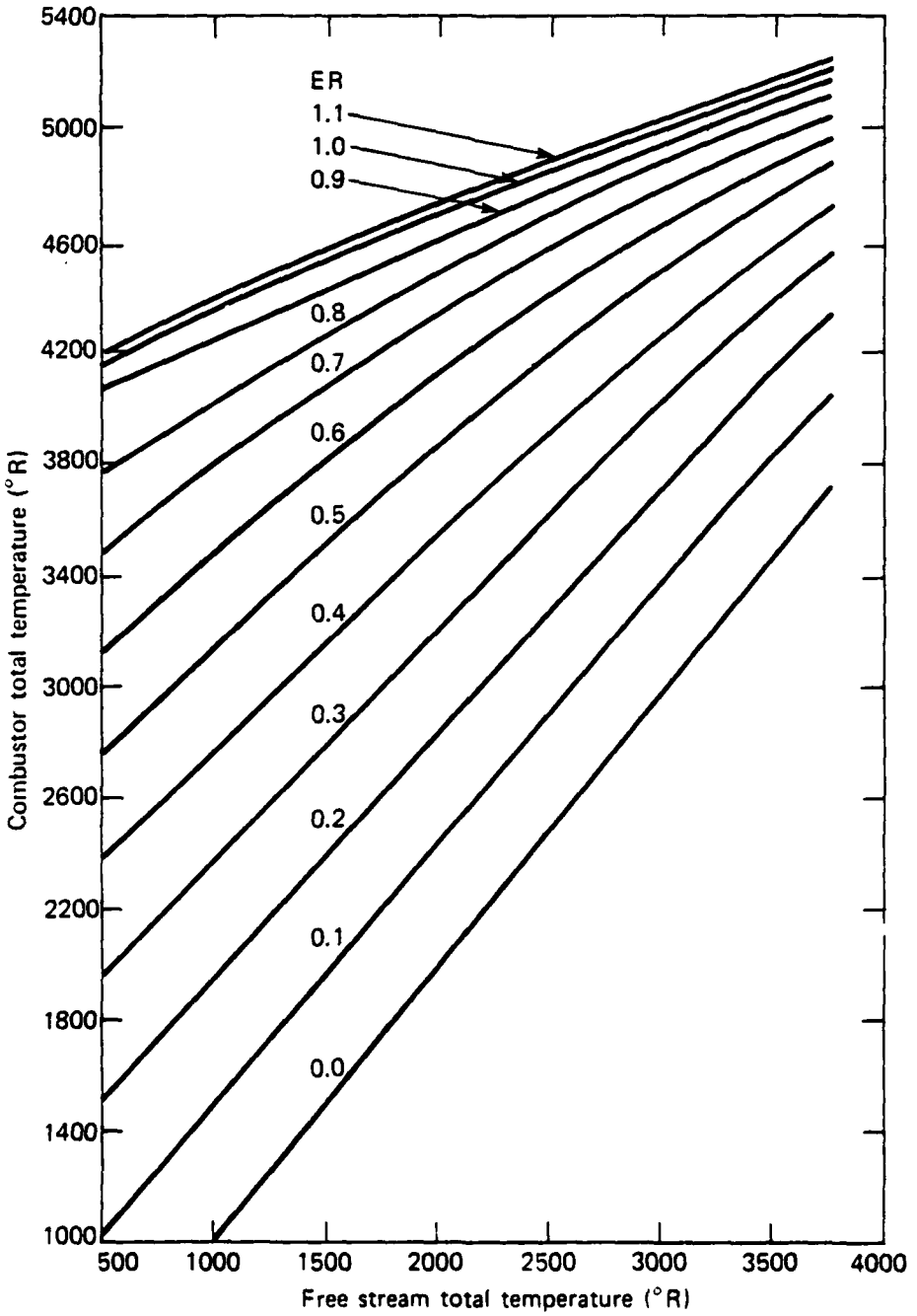

Fig. A-2 Combustor T_t versus free stream T_t, Shelldyne - H.


DA
FIL